Catalysis Today 159 (2011) 2–11

Contents lists available at ScienceDirect

Catalysis Today

journal homepage: www.elsevier.com/locate/cattod

Development of metal nanoparticles supported materials as efficient catalysts for reductive amination reactions using high-throughput experimentation

Marcelo E. Domine[a,*], M. Consuelo Hernández-Soto[a], Yolanda Pérez[b]

[a] Instituto de Tecnología Química (UPV-CSIC), Universidad Politécnica de Valencia, Consejo Superior de Investigaciones Científicas. Avda. de los Naranjos s/n, 46022, Valencia, Spain
[b] Universidad Rey Juan Carlos, Tulipán s/n, 28933, Móstoles, Madrid, Spain

ARTICLE INFO

Article history:
Available online 25 September 2010

Keywords:
Reductive amination
Multi-functional catalysts
Metal catalysts
Metal nanoparticles
HT experimentation

ABSTRACT

Substituted amines and N-heterocycles, useful intermediates in industry, can be synthesized by reductive amination of ketones with amines in the presence of metal supported catalysts. In this work, multi-functional catalysts based on Pt, Pd, and Au nanoparticles supported on different metal oxides capable to efficiently catalyze the liquid phase selective reductive amination of ketones have been developed. Catalytic screening performed by HT experimentation showed that Pt-catalysts are more active than the corresponding Pd counterparts, while Au-based materials present very low activities. Excellent results were obtained with Pt/TiO_2 (52% of amine conversion with selectivity >95%, TON = 2033) followed by Pt/MgO, Pt/CaO, and also Pt/Al_2O_3. Increase in the reduction temperature pre-treatment of Pt-catalysts improved the catalytic activities (≈65% of amine conversion with selectivity >95%, TON = 2541 for Pt/TiO_2), these values being quite superior to those observed with Pt/C and Pt/Al_2O_3 commercial catalysts. With the appropriate treatment of support prior to metal impregnation efficient Pt/Al_2O_3 materials can also be obtained (TON = 1685). The results suggest that Pt and Pd catalysts activities can be enhanced by appropriate tailoring the physical and chemical properties of oxide supports depending on the type of metal, this favouring a strong metal-support interaction (SMSI) on solids.

1. Introduction

The reductive amination of alcohols and ketones, also known as N-alkylation of amines with alcohols and ketones, is a widely used organic reaction for the synthesis of substituted amines [1] and several both aromatic and aliphatic N-heterocycles, such as pirazines and piperazines, respectively [2–5]. The later are useful intermediates for the preparation of pharmaceutical, agro-chemicals, and perfumery products. In general, these nitrogen compounds are commonly synthesized by reduction of the corresponding (di)ketopiperazines or by various cyclization reactions, for example, by dialkylation of amines with bis(2-chloroethyl)amine, or by intramolecular reductive coupling of diamines [6,7]. Moreover, they can also be prepared by multi-step reactions involving consecutive addition, cyclization, and reduction (consecutive reductive amination process) of alcohols, aldehydes or ketones with ammonia in the presence of metal supported and solid acids catalysts [2–5].

In the reductive aminations, the use of aldehydes or ketones is generally preferred to the alcohols due to the low reactivity presented by the later [8]. In the case of carbonyl compounds, the process takes place in several steps (Scheme 1) [8] including: (i) addition and generation of the hemi-aminal intermediate, (ii) dehydration and formation of the imine or enamine intermediate (depending on the primary or secondary starting amine used, respectively), and (iii) imine or enamine reduction for the final substituted amine production. The overall process requires redox metallic active sites, and additionally acid–base centres of moderate strength [9,10]. The most commonly used catalysts for the reductive aminations of aldehydes or ketones with amines are mixed metal oxides and metal modified-zeolites (metal = Cu, Zn, Ni, and Co) [2–5,8]. In the case of alcohols, the reaction mechanism proposed for these reactions mediated by metal oxides and Me-zeolites includes a first step of oxidative dehydrogenation of the alcohol to the corresponding carbonyl compound [8,9], this being the determinating reaction step. This fact explains the low reactivity and the elevated temperatures needed to obtain the desired substituted amines starting from the alcohols. It has been reported Ru(II) and Ir(I) homogeneous complexes [11–13], as well as Ni-Raney [14], as catalysts for the reductive aminations with alcohols performed at high H_2 pressures and temperatures, but in these cases the yields are moderate to low whereas the catalyst recover is problematic.

When aldehydes and ketones are used as reactants, the hydrogenation of enamine or imine intermediates is the slowest step of

* Corresponding author. Tel.: +34 963879696; fax: +34 963877809.
E-mail address: mdomine@itq.upv.es (M.E. Domine).

0920-5861/$ – see front matter © 2010 Elsevier B.V. All rights reserved.
doi:10.1016/j.cattod.2010.08.011

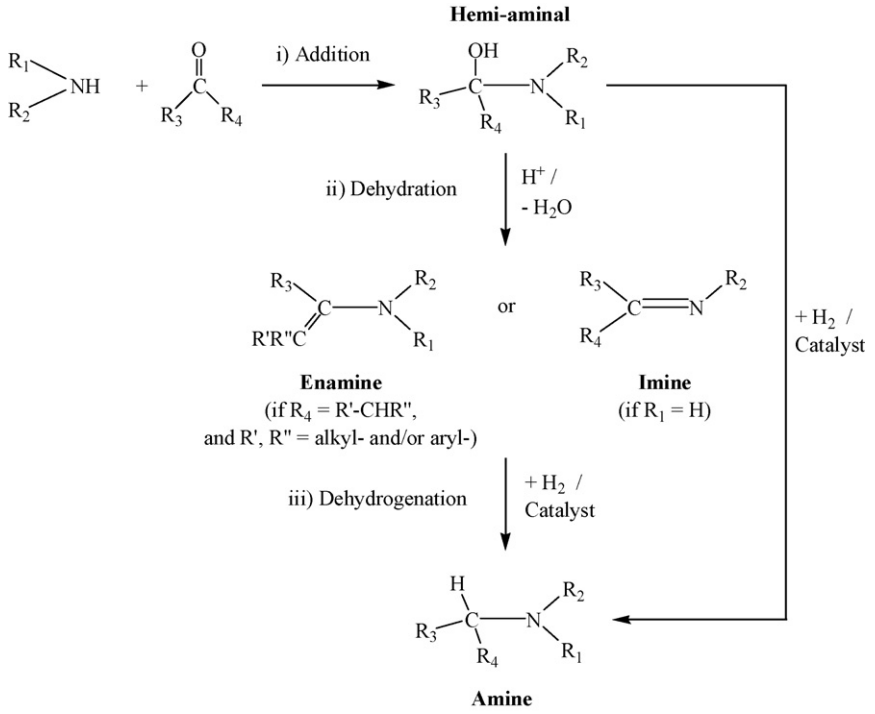

Scheme 1. Reaction steps and intermediates proposed in the reductive amination of carbonyl compounds.

the process, this being the reason for working under H_2 addition at moderate to high temperature during reaction [15]. Under these conditions, the hydrogenation of the carbonyl group competes with the imine or enamine reduction decreasing the selectivity of the process. Some organo-metallic homogeneous catalysts [16,17], and also Pd and Ni complexes supported on silicates and alumino-silicates [18] are able to selectively reduce C=C and C=N functionalities in the presence of C=O groups under moderate reaction conditions. Nevertheless, many drawbacks concerning the handling of the catalytic precursors and the recycling of catalysts limit their widespread application. If the objective is to carry out the reductive amination under mild reaction conditions, metal active sites capable to perform the imine or enamine selective reduction by working at low temperatures and H_2 pressures are needed. In this sense, we have considered that controlled size metal nanoparticles (i.e. Pt, Pd, Ru, and Au) supported on solid materials can dissociate the H_2 molecule at low temperature and, importantly, when H_2 is present on the catalytic surface in low concentrations. Moreover, if solid supports with adequate acid–base properties, high surface area, and controlled particle size and porosity are selected, it could be possible to design effective and selective multi-functional catalysts for the reductive amination process.

In this work, we have prepared several catalytic materials based on Pt, Pd, and Au nanoparticles supported on different metal oxides, such as Al_2O_3, CeO_2, TiO_2, ZnO, ZrO_2, MgO, and CaO. Their synthesis and characterization will be described, whereas their rapid catalytic screening in the reductive amination of ketones under mild reaction conditions in the absence of solvent by using high-throughput (HT) experimentation will also be depicted. The influences of the type of metal, and both acid–base and textural properties of supports on the catalytic activities will be studied, these activities being compared with commercial catalysts and other Me-supported materials commonly used in this process. Thus, the combination of rational design of catalysts together with the rapid screening of the different prepared materials by HT experimentation lead us to select the most adequate multi-functional catalytic materials to be further studied and optimised for the development of effective catalysts in the reductive amination reaction.

2. Experimental

2.1. Materials

Cyclohexanone (99.8%), 2-hexanone (98%), 2-octanone (98%), piperidine (99%), and *n*-nonane (99%) were purchased from Sigma–Aldrich and used as received. Acetone, acetonitrile, 2-propanol (Scharlau, analytical grade, 99.5%), and water (Milli-Q quality, Millipore) were used as solvents, whereas hydrogen 5.0 (Abelló Linde S.A., 99.999%) was used as reduction agent. MgO (NanoActive Plus, surface area $\geq$300 m^2/g), CaO (Aldrich, 98%, surface area $\approx$160 m^2/g), ZnO (Aldrich, Reagent Plus® 99.9%, surface area $\approx$70 m^2/g), ZrO_2 (Aldrich, 99%, surface area $\approx$45 m^2/g), and TiO_2 (Merck, surface area $\approx$50 m^2/g) were employed as supports in their powder form. $Pd(NH_3)_4{\cdot}6H_2O$ (Aldrich, 99.99+%), $H_2PtCl_6{\cdot}6H_2O$ (Aldrich, $\geq$37.5% Pt basis), and $HAuCl_4{\cdot}3H_2O$ (Aldrich, 99%) were used as metal sources.

For comparative purposes the following commercial catalysts supplied by Aldrich were also used: 5 wt% Pt/C, 5 wt% Pd/C, 5 wt% Pt/Al_2O_3, and 5 wt% Pd/Al_2O_3. Additionally, 2.5 wt% Au/C [Johnson Matthey, M04438] and 1.5 wt% Au/TiO_2 [World Gold Council, #02-04-WG-C] standard catalysts were also used.

2.2. Catalysts preparation

2.2.1. Synthesis of high surface γ-Al_2O_3 and meso-structured CeO_2

The amorphous γ-Al_2O_3 (surface area > 300 m^2/g) was synthesized following the procedure detailed in the literature [19]. The obtained gel was treated by lyophilisation [L] and/or calcination in air at 500 °C [C5], and 800 °C [C8] to evaluate the influence of support pre-treatment in the catalytic activity of final metal-supported catalysts.

Synthesis of meso-structured CeO_2 (surface area ≈200 m^2/g) was performed following the procedure reported in ref. [20]. The CeO_2 support was calcined at 450 °C in air before use.

2.2.2. Pd and Pt incorporation on different metal oxides as supports

In general, metal incorporation on different previously calcined metal oxides was performed by the incipient wetness impregnation method using aqueous solutions of $Pd(NH_3)_4{\cdot}6H_2O$ and $H_2PtCl_6{\cdot}6H_2O$ as Pd and Pt sources, respectively. The solid samples were dried in oven at 100 °C overnight, and then calcined at the corresponding temperature above-mentioned depending on the type of support used. The thus obtained catalytic materials were activated under H_2 flow (100 ml/min) at 350 °C during 3 h before use. Metal loadings on solids were determined by chemical analyses (ICP), whereas metal nanoparticles size and distribution on different supports were measured by TEM.

2.2.3. Au deposition on different supports

Deposition of gold on CeO_2 support was carried out by a deposition–precipitation method with $HAuCl_4{\cdot}3H_2O$ as the source of Au, following the experimental procedure detailed in [21,22]. Incorporation of gold nanoparticles onto ZnO, ZrO_2, and TiO_2 surfaces was similarly performed by adaptation of the deposition–precipitation method above-mentioned.

Deposition of gold nanoparticles onto CaO was performed as follows: a solution of NaOH (0.2 M) was added to 0.178 g of $HAuCl_4{\cdot}3H_2O$ diluted in 20 ml of water (Milli-Q quality) until a pH 10 was reached. This Au salt in water solution (pH 10) was added to a container holding 2.0 g of CaO in 30 ml of water, under continuous agitation. The mixture was then stirred at room temperature during 18 h. Once the solid had been recovered by filtration, it was washed thoroughly with water and oven dried at 100 °C for approximately 12 h. In the case of MgO, the NaOH solution (0.2 M) was added to 0.3 g of $HAuCl_4{\cdot}3H_2O$ diluted in 35 ml of water until a pH 7–8 was reached. This Au salt solution (pH 7–8) was added to a container holding 2.85 g of MgO in 100 ml of water at 70 °C, under continuous agitation. The mixture was continuously stirred at 70 °C during 1 h, and then stirred at room temperature during 16 h. From this point the followed procedure was identical to that used with CaO as a support. Gold contents on solids were determined by XRF and chemical analyses of samples.

The Au containing samples were used as catalysts as synthesized [AS], as well as after reduction either under H_2 flow (100 ml/min) at 350 °C during 3 h [HR] or with phenyl ethanol solution (10 ml/g of solid) in a batch reactor at 160 °C during 2 h [AR]. In the later case, the recovered solid was consecutively washed with acetone and diethyl ether, and then dried at 100 °C overnight.

2.3. Catalysts characterization

Phase purity of the catalysts was determined by X-ray diffraction (XRD) in a Philips X'Pert MPD diffractometer equipped with a PW3050 goniometer (CuKα radiation, graphite monochromator), provided with a variable divergence slit and working in the fixed irradiated area mode. Diffuse reflectance UV–vis (DRUV) spectra of samples were recorded in a Cary 5 Varian spectrometer equipped with a "Praying Mantis" cell from Harrick.

Thermogravimetric and differential thermal analyses (TGA–DTA) were performed in a Netzsch STA 409 EP thermal analyzer with about 20 mg of sample and a heating rate of 10 °C min^{-1} in air flow (6 l h^{-1}). Surface area, pore volume, and pore size distribution of the solid samples (200 mg) were calculated by the BET method by carrying out liquid nitrogen and argon adsorption experiments at 77 and 85 K, respectively, in a micromeritics flowsorb apparatus. Chemical composition was determined by using an inductively coupled plasma emission spectrophotometer Varian 715-ES and elemental analyses in a Fisons EA1108CHN-S. Au content on solids was determined by X-ray fluorescence spectroscopy (Philips MiniPal 25 fm spectrometer). Samples for transmission electron microscopy (TEM) were ultrasonically dispersed in ethanol and transferred to carbon coated copper grids. TEM micrographs were collected in a Philips CM-10 microscope operating at 100 kV. Average particle size values were obtained by measuring the diameters of about 100 particles in a representative region.

2.4. High-throughput catalytic testing

Catalytic experiments were performed in SPR16 apparatus from AMTEC possessing 16 slurry parallel reactors (12 ml stainless steel autoclave reactors), individually equipped with a magnetic bar, and sensors for both temperature and pressure control. The reactors have also individual connections to allow gas supply, and also an outlet for samples to be taken at different time intervals. Typically, equimolecular amounts of piperidine (18 mmol) and the selected ketone (18 mmol) were placed into the reactor followed by catalyst addition (90–100 mg of solid). The autoclave was hermetically sealed, pressurised with hydrogen at 5 bars (free volume between 6.2 and 6.7 ml depending on selected ketone used), and heated at reaction temperature (100 °C), under continuous stirring. Small liquid aliquots (≈100 μl) were taken, filtered off and diluted in 0.5 g of a iso-propanol solution containing 2 wt% *n*-nonane as standard. The liquid samples were analysed by a 3900-Varian GC equipped with both a FID detector and a capillary column (HP-5, 30 m length). Products identification was done by GC–MS (Agilent 6890N GC System coupled with an Agilent 5973N mass detector) by comparison with commercially available standard, and also by liquid ^1H and ^{13}C NMR spectroscopy.

Amine (and also ketone) conversion and selectivities of products (based on GC obtained data) are defined as: (initial moles of reactant – final moles of reactant)/initial moles of reactant × 100 and moles of product *i*/moles of total products × 100, respectively. Turnovers number (TON) here reported is defined as: moles of products/moles of metal on solid.

3. Results and discussion

3.1. Commercial catalysts preliminary evaluation (effect of the type of ketone)

Initially, in order to establish the optimal reaction conditions to be applied in the HT experimentation study, a rapid evaluation of commercial catalysts based on Pd, Pt, and Au catalysts supported on C, Al_2O_3, and also TiO_2 was performed. In these experiments, piperidine (a secondary amine) as nitrogen providing compound and cyclohexanone were mixed in equimolecular amounts (18 mmol) with 90 mg of catalyst in the absence of solvent. As can be seen in Fig. 1(A), excellent levels of amine conversion were achieved with Pd-based commercial catalysts (5 wt% Pd/C and 5 wt% Pd/Al_2O_3), while rather lower conversion values were obtained with Pt-based catalysts (5 wt% Pt/C and 5 wt% Pt/Al_2O_3). Nevertheless, these differences are not so surprising if we consider that the moles of Pd on solids are practically two-fold the moles of Pt. Calculations of TON (moles of products/moles of metal on catalyst) revealed that Pd and Pt commercial catalysts showed very similar catalytic activities (Figs. 1(A) and 2). Additionally, both Pd and Pt commercial catalysts presented selectivity values to the desired tertiary amine product higher than 85%, this being particularly interesting in the case of Pd/Al_2O_3 catalyst with a selectivity of 100% (Fig. 1(B)).

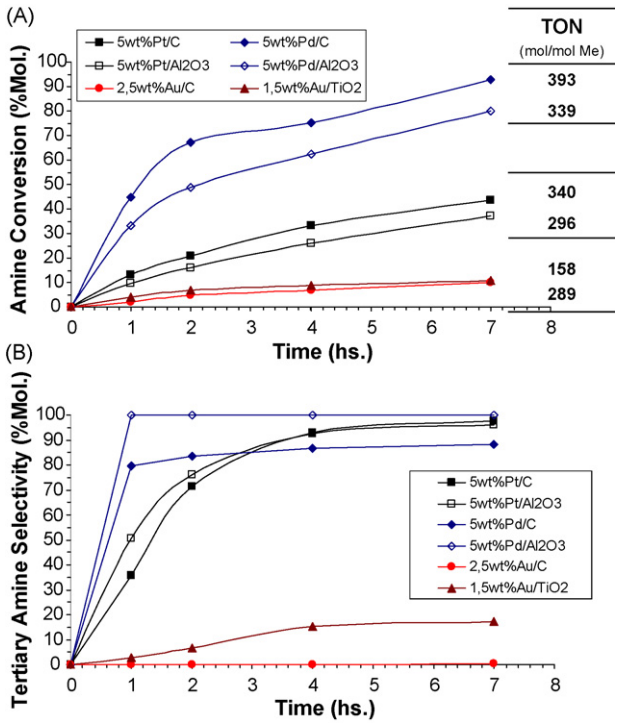

Fig. 1. Catalytic activity of Pd, Pt, and Au commercial catalysts in the reductive amination of cyclohexanone with piperidine (at 100 °C and P_{H_2} = 5 bar during 7 h); (A) amine conversion (%mol.), and (B) selectivity to tertiary amine (%mol.).

In the case of the gold-based materials, quite low amine conversion as well as poor tertiary amine selectivities were encountered with both 2.5 wt% Au/C and 1.5 wt% Au/TiO_2 catalysts tested (Fig. 1).

The Pd, Pt, and Au-based commercial catalysts were also tested in the reductive amination reaction by using piperidine and 2-octanone or 2-hexanone as reactants under similar reaction conditions than those used for cyclohexanone. As can be seen in Fig. 2, the catalytic activities (TON, mol/mol^{-1}) observed with all the catalysts by using both linear ketones were lower to those obtained with cylohexanone, except with the 5 wt% Pt/C catalyst. From these results it can also be concluded that Pd-based catalysts showed to be quite sensible to the ketone structure, this effect being not observed in the case of Pt-catalysts. As cyclohexanone was in general found the most reactive ketone, we decided to use piperidine and cyclohexanone as reactants for the model reductive amination reaction in this study.

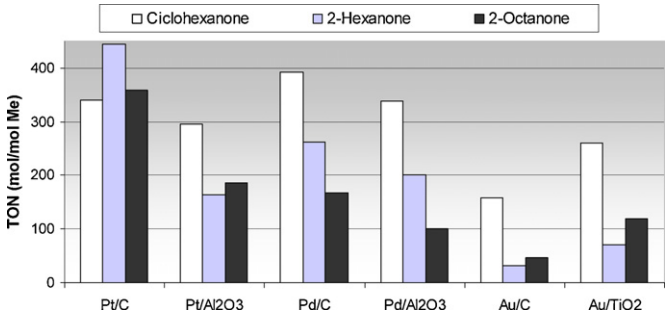

Fig. 2. Catalytic activity (TON, mol mol^{-1}) of Pd, Pt, and Au commercial catalysts in the reductive amination of ketones with piperidine (at 100 °C and P_{H_2} = 5 bar, values calculated at 7 h of reaction).

3.2. Catalytic screening using HT experimentation

The selective reductive amination of cyclohexanone with piperidine (model reaction) was first studied using HT experimentation by performing a rapid screening of several tailored catalysts prepared in this work based on Pd, Pt, and Au nanoparticles supported onto different metal oxides. High surface area CaO and MgO, specially prepared γ-Al_2O_3 and CeO_2, and also ZnO, ZrO_2, and TiO_2 were selected as supports. Amine conversion (Fig. 3(A)), tertiary amine selectivity (Fig. 3(B)) and catalytic activity per metallic center on solid (TON, mol/mol^{-1}, Fig. 3(C)) were taken into account for the evaluation of different catalysts, the TON being used as the primer selection criteria followed by tertiary amine selectivity. The main textural and physical properties of Pt and Pd nanoparticles supported catalysts presenting the best catalytic performances in this rapid screening with the help of HT experimentation are summarized in Table 1. Additionally, catalytic results concerning amine conversion, *tert*-amine selectivity and TON values are also provided in the table for comparison.

As can be seen in Fig. 3 (and also in Table 1), the best results in amine conversion (52%) and TON (2033) were obtained with Pt/TiO_2 catalysts, this sample also allowing excellent tertiary amine selectivity (98%). Other Pt-catalysts, such as Pt/MgO (TON = 1706), Pt/CaO (TON = 1528), and Pt/Al_2O_3 (TON = 885) had good catalytic activities with high *tert*-amine selectivities (≥95%) whereas moderate both TON (706) and *tert*-amine selectivity (61%) values were observed with Pt/ZrO_2. Moreover, Pt supported on ZnO and ZrO_2 materials showed very low TON values (≈550) with the lowest *tert*-amine selectivity values of the series. Thus, the reactivity order encountered with the Pt-based solid catalysts here prepared was: Pt/TiO_2 > Pt/MgO >, Pt/CaO ≫ Pt/Al_2O_3 > Pt/ZrO_2 ≫ Pt/ZnO ≈ Pt/CeO_2.

In the case of Pd-catalysts (Fig. 3 and Table 1), the reactivity order was completely different to that observed with Pt-based samples. In this sense, Pd/CaO and Pd/Al_2O_3 catalysts showed the higher TON values (1294 and 924, respectively) of the series, in both cases *tert*-amine selectivity levels around 98% were achieved. Besides, Pd/CeO_2, Pt/ZrO_2, and Pd/TiO_2 materials showed moderate amine conversion and acceptable *tert*-amine selectivity values, while Pd supported on MgO and ZnO presented the lowest catalytic results of the series. From these results, the following reactivity order for Pd-catalysts was established: Pd/CaO > Pd/Al_2O_3 ≫ Pd/CeO_2 ≈ Pd/ZrO_2 > Pd/TiO_2 > Pd/ZnO ≫ Pd/MgO.

As it was expected, Au-based catalysts showed the worst amine conversion and TON values, but more importantly, quite low to negligible amounts of tertiary amine were produced in all the cases. These results confirmed those already observed and commented with gold commercial catalysts (see Figs. 1 and 2 in Section 3.1.) concerning the low activity of Au nanoparticles for this reductive amination process. Moreover, neither the use of as synthesized Au supported catalytic samples [AS] nor the special reduced with phenylethanol Au supported samples [AR] were able to enhance the catalytic activities observed when comparing with that obtained using standard reduced Au supported samples [HR] as catalysts (Table 2).

In light of the HT experimentation results, it was clearly concluded that Pt-based materials, specifically Pt/TiO_2, Pt/MgO, Pt/CaO, and Pt/Al_2O_3 were the most adequate catalysts for the amination reductive process, while in the case of Pd-catalysts only Pd/CaO and Pd/Al_2O_3 samples were sufficiently active and selective. It is worth noting that the extraction of some profitable trends or tendency from the above-mentioned results related to the catalytic activity observed and the type of support used for each Pt-catalysts, and also for Pd samples, is not straight forward (See supporting information).

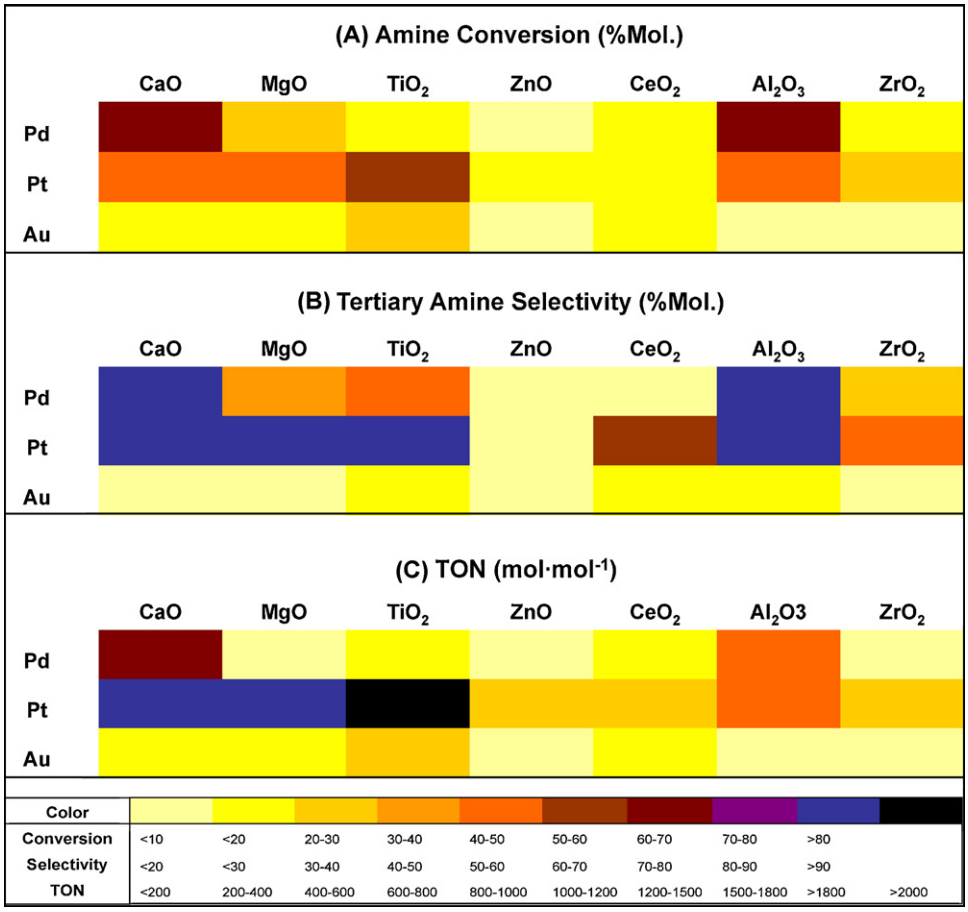

Fig. 3. Catalytic behaviour diagrams of metal supported materials in the reductive amination of cyclohexanone with piperidine (at 100 °C and P_{H_2} = 5 bar during 7 h–catalysts reduced at 350 °C); (A) amine conversion, (B) selectivity to tertiaty amine, and (C) TON (mol mol^{-1}).

Table 1
Main physical, textural, and catalytic properties of Pt and Pd catalysts using different metal oxides as supports.

Catalyst	Metal (wt%)[a]	Me particle size (nm)[b]	Surface area (BET) (m^2/g)	Conversion (%mol.)[c]	Tert-amine selectivity (%mol.)[c]	TON (mol/mol Me)[c]
Pt/TiO_2	1.0	3	39	52	98	2033
Pt/MgO	1.1	5–6	74	48	97	1706
Pt/CaO	1.1	3–4	49	43	95	1528
Pt/Al_2O_3	1.5	4–5	220	43	95	885
Pd/TiO_2	1.0	4–5 (≈20)[d]	29	11	55	233
Pd/MgO	1.0	2–3	57	4	44	89
Pd/CaO	1.0	4–6	53	61	98	1294
Pd/Al_2O_3	1.4	5	285	48	98	727

[a] wt% of metal measured by inductively coupled plasma emission spectrophotometry (ICP).
[b] Calculated as the medium value from transmission electron microscopy (TEM) data.
[c] Reductive amination model reaction at 100 °C and P_{H_2} = 5 bar during 7 h (catalysts reduced at 350 °C during 3 h under 100 ml/min H_2 flow before reaction).
[d] Most of the particles diameters centred at 4–5 nm and a minor amount of particles at ≈20 nm.

Table 2
Effect of Au-catalysts reduction treatments on the catalytic activity observed in the reductive amination of cyclohexanone with piperidine (at 100 °C and P_{H_2} = 5 bars during 7 h).

Catalyst [Reduction treatment][a]	Me particle size (nm)[b]	Conversion (%mol.)	Selectivity (%mol.)		TON (mol/mol Me)
			Enamine	*tert*-Amine	
2.5 wt%Au/CeO_2 [AS]	<4	9	72	24	142
2.5 wt%Au/CeO_2 [HR]	<4	14	68	29	221
2.5 wt%Au/CeO_2 [AR]	<4	14	73	25	221
1.4 wt%Au/MgO [AS]	4–5	16	98	0.2	315
1.4 wt%Au/MgO [HR]	4–5	13	97	0.4	256
3.2 wt%Au/CaO [AS]	4–5	6	91	4	118
3.2 wt%Au/CaO [HR]	4–5	12	96	1	236

[a] Reduction treatments before reaction: [AS],as synthesized; [HR],at 450 °C under 100 ml/min H_2 flow during 3 h, [AR],with phenylethanol at 160 °C during 2 h.
[b] Calculated as the medium value from transmission electron microscopy (TEM) data.

Thus, non-linear dependence of catalytic results of all Pt and Pd supported on different oxide materials have been here found with respect to different support properties, such as surface area, pH, and even the atomic number (Z), electronegativity (E), or effective ionic radii of metal component of oxides (See supporting information). Nevertheless, two well-defined groups of Pt supported materials have been encountered when the pH and the effective ionic radii of metal component of oxides were taken into account (see Figs. S1 and S5 in supporting information). The first group included TiO_2 (neutral, pH ≈6.2), and both MgO and CaO basic oxides (pH ≈10.3 and 11.8, respectively), they having pH measured values ≥6.2. The second group was formed by the most acidic supports (pH measured values <6.2) including γ-Al_2O_3, CeO_2, ZrO_2, and ZnO. When Pt was supported on the later group of oxides, the obtained materials were the less active catalyst for reductive amination reaction, γ-Al_2O_3 showing the highest catalytic activity and selectivity of the series. On one hand, it could be clearly inferred that the acid/base character of oxide support have a great influence on the Me-catalyst activity. On the other hand, the unlike metal-support interactions in each group of Me-catalysts probably determine the H_2 dissociation capacity of the Pt (or Pd) supported nanoparticle, and consequently, the catalytic efficiency for the reductive amination reaction. In this sense, the most promising prepared Pt-catalysts, preferably those with high catalytic activities and selectivities (i.e. Pt/TiO_2, Pt/MgO, Pt/CaO, and Pt/Al_2O_3), were selected for further investigations. Detailed physico-chemical characterizations together with further catalytic experiments of the selected Pt-catalysts were performed in order to elucidate the different properties of the solid materials and their influences on the observed catalytic activity. In principle, this knowledge could facilitate us the understanding of the catalytic reaction on solid surface providing the scientific bases for the enhancement of catalytic behaviour by adequate modifications of catalysts.

3.3. Study and catalytic activity enhancement of Pt supported catalysts

Firstly, the most efficient Pt-based materials selected after HT catalytic screening, such as Pt/TiO_2, Pt/MgO, and Pt/CaO, were structurally studied and compared with the corresponding Pd counterparts for each support oxide. Fig. 4(A) shows the experimental XRD patterns of Pt/and Pd/TiO_2 reduced samples, as well as the diffractogram of calcined support corresponding to anatase titania. The presence of Pt metallic species in the Pt/TiO_2 reduced catalyst was inferred by the low intensity reflections peaks at $2\theta = 39.9$, 46.7, 67.8, 81.8, and 86.0 [23]. TEM micrographs of this Pt/TiO_2 sample confirmed the presence of homogeneously dispersed Pt nanoparticles of 3 nm diameters with a narrow distribution (Fig. 5(A)). In the case of Pd/TiO_2 reduced sample, a double Pd particle size distribution was encountered by TEM measurements, most of the particles presenting average diameters of around 4–5 nm with a minor amount of them centred at 20–22 nm (Figs. S10A and S12A in supporting information), although only one reflection peak at $2\theta = 40.1$ assigned to Pd^0 species was found in the Pd/TiO_2 XRD diffractogram. In both Pt- and Pd-supported on TiO_2 materials, the anatase titania structure remained almost unaltered.

The X-ray diffraction patterns of Pt and Pd supported on CaO materials are shown in Fig. 4(B). The characteristic reflections peaks of calcium oxide were observed in the diffractogram of calcined support [24], but an evident change mainly to the corresponding $Ca(OH)_2$ phase appeared after metal incorporation in both Pt- and Pd-based samples. The Pt/CaO reduced catalyst possessed the very weak reflections peaks characteristic of Pt metallic species, this being corroborated by TEM measurements with the presence of ≈4 nm Pt nanoparticles relatively well dispersed onto the support (Fig. 5(B)). XRD patterns (Fig. 4(B)) and TEM images

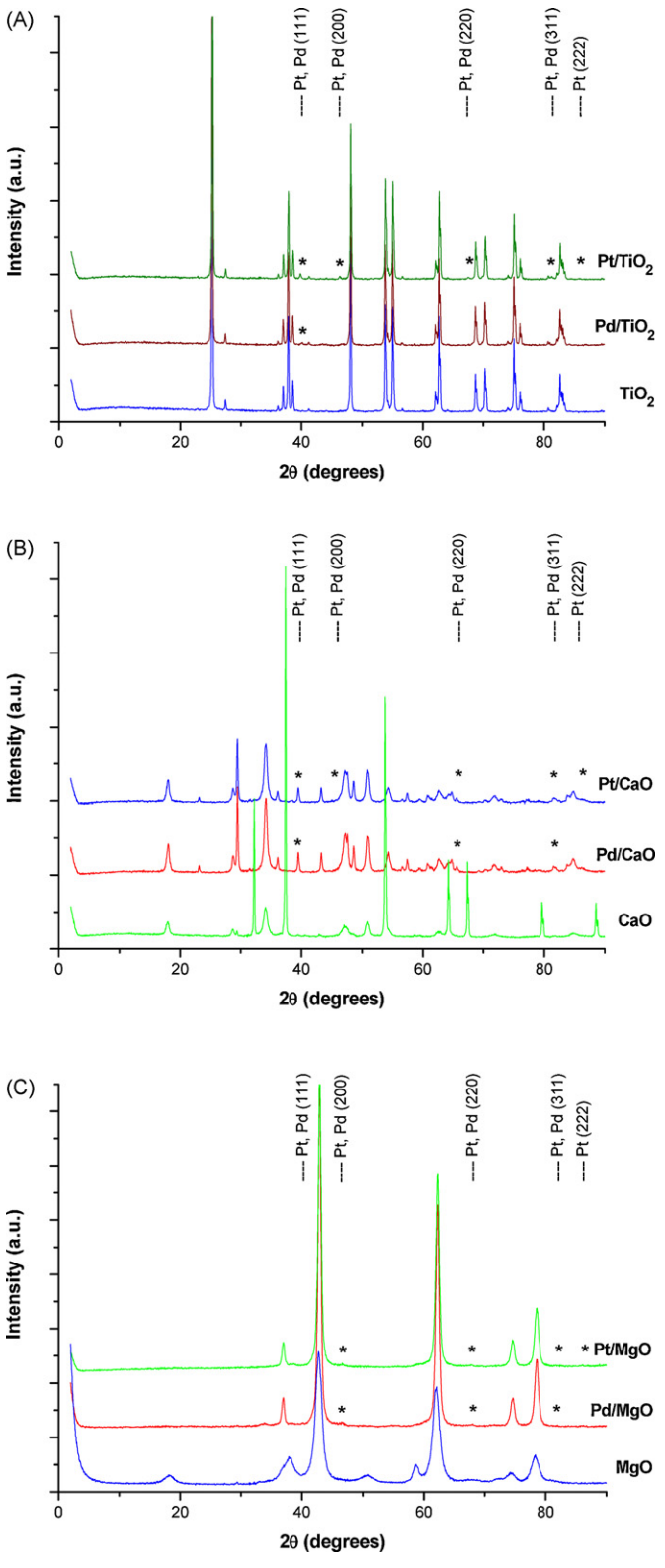

Fig. 4. XRD patterns of Pt and Pd nanoparticles supported on: (A) TiO_2, (B) CaO, and (C) MgO (reduced samples).

(Fig. S10B in supporting information) of the Pd/CaO reduced sample also confirmed the existence of Pd nanoparticles in the solid.

As can be seen in Fig. 4(C), the XRD pattern of calcined MgO used as support showed the presence of the expected MgO periclase phase together with ≈20% $Mg(OH)_2$ brucite phase [25,26]. Nevertheless, both Pt and Pd supported on MgO reduced samples

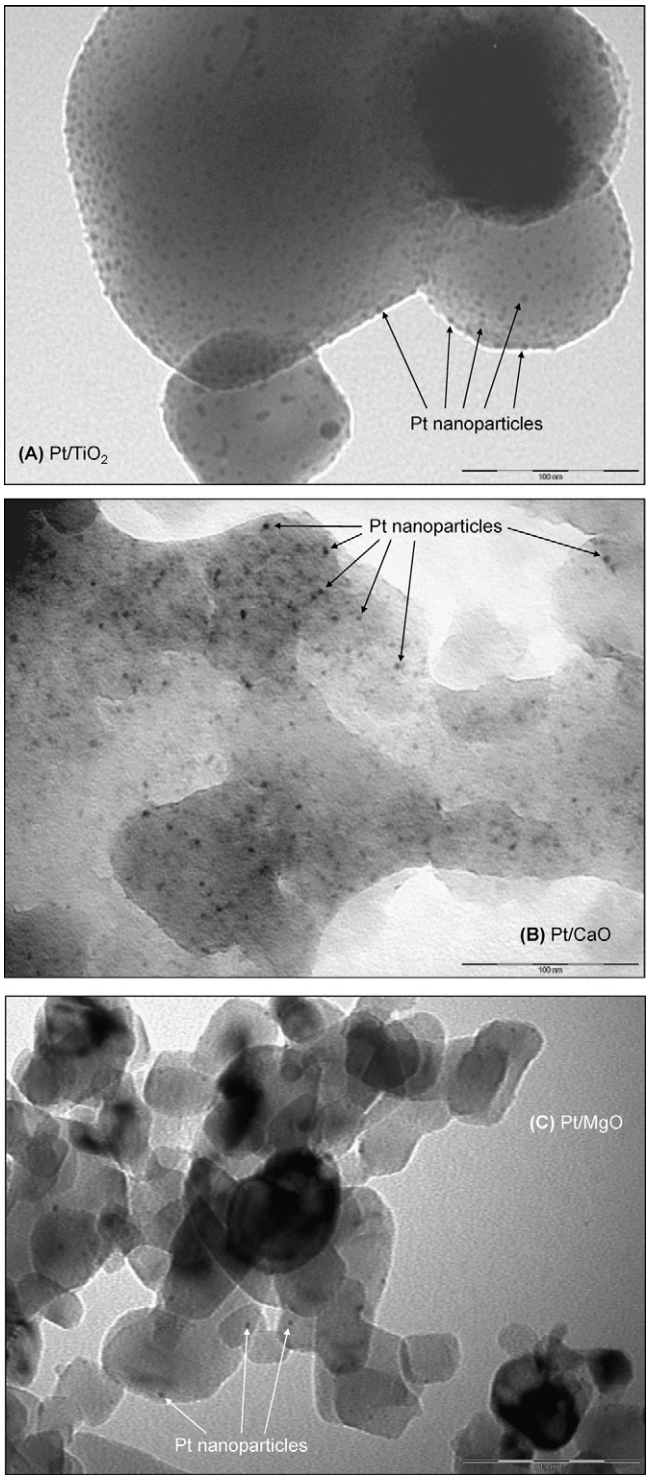

Fig. 5. TEM micrographs of Pt/TiO_2 (A), Pt/CaO (B), and Pt/MgO (C) catalysts (reduced samples).

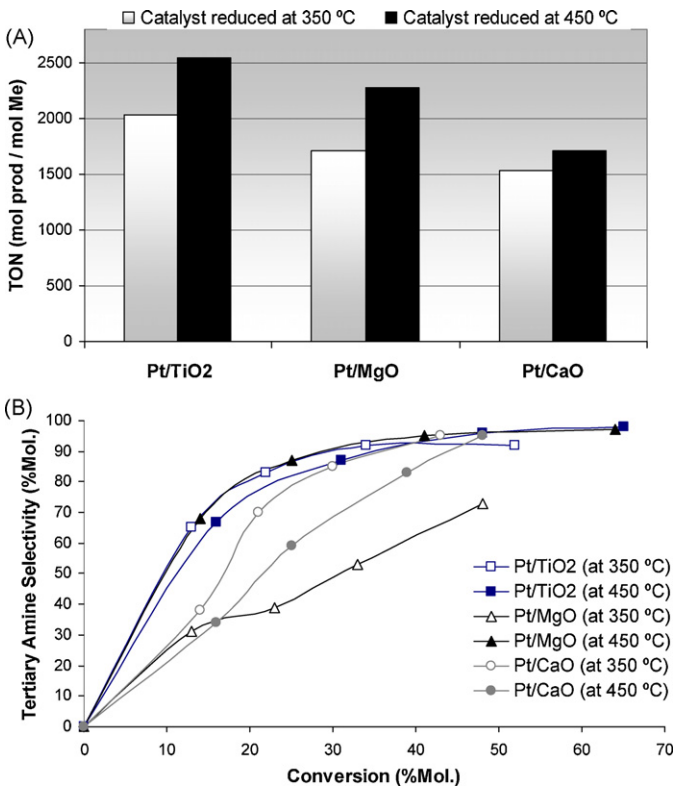

Fig. 6. Effect of reduction treatments on the catalytic activity observed in the reductive amination of cyclohexanone with piperidine over Pt-catalysts (at 100 °C and P_{H_2} = 5 bar during 7 h); (A) TON (mol mol^{-1}), and (B) tertiary amine selectivity vs. conversion (%mol.).

only presented the reflections peaks characteristic of MgO periclase phase, the $Mg(OH)_2$ containing being practically negligible. Of course, the reflections peaks corresponding to the presence of Pt^0 and Pd^0 species were clearly distinguished in Pt/and Pd/MgO reduced samples, respectively. Once again, the existence of well-defined Pt and Pd nanoparticles with a narrow distribution on the MgO support surface was confirmed by TEM measurements in both cases (Fig. 5(C) and Fig. S10C for Pt- and Pd-based materials, respectively).

It is well known in the literature [25–28] that optimal noble metal reduction temperature change depending on the type of oxide support involved due to the different metal-support interactions taking place in each case. Following this idea, we studied the influence of reduction pre-treatment temperatures on the catalytic behaviour of Pt-catalysts. The results obtained in the reductive amination model reaction by performing the reduction treatment of Pt-catalysts before catalytic experiment at 350 and 450 °C are shown in Fig. 6. In general, the higher reduction temperature the better catalytic performance was observed, this being true for the three oxide supports here studied. Thus, Pt/TiO_2 sample showed an increase in the catalytic activity (TON calculated at 7 h of reaction from 2033 to 2541, Fig. 6(A)) when reduction temperature was augmented from 350 to 450 °C, selectivity to the tertiary amine remaining practically constant (>95%). A quite better behaviour was observed in the case of Pt/MgO sample increasing the TON values from 1706 to 2274 when reduction temperature was augmented in 100 °C (from 350 to 450 °C) whereas *tert*-amine selectivity was also improved from ≈70% to >95% in this case. Finally, Pt/CaO sample also showed a slightly increase in the catalytic activity (TON values from 1528 to ≈1700) with the augmentation of reduction temperature, also accompanied with a decrease in the selectivity to the *tert*-amine mainly observed at low conversion levels (Fig. 6(B)). Generally speaking, it is possible that a small increase in the catalytic activity observed with Pt-catalysts after 450 °C pre-reduction could be due to the further reduction of Pt oxide species present in the solids in very small quantities. This contribution could not be ruled out, but it is not enough to clarify the differences in catalytic results observed in Fig. 6. Thus, the enhancement of the Pt-catalysts catalytic activity observed can be explained by an improved metal-support interaction with increasing reduction temperature, this strong metal-support interaction (SMSI) [29,30] facilitating H_2

Table 3
Main physical and textural properties of Pt/Al_2O_3 materials prepared by using different pre-treatments of support.

Sample	Metal (wt%)[a]	γ-Al_2O_3 pre-treatment	Me particle size (nm)[b]	Surface area (BET) ($m^2\ g^{-1}$)
1Pt/Al [L]	1.0	Lyophilisation	4–5	400
1Pt/Al [C8]	1.0	Calcination at 800 °C	4–5	228
2Pt/Al [C8]	2.0	Calcination at 800 °C	4–5	220
1Pt/Al [C5]	1.0	Calcination at 500 °C	4–5	335
2Pt/Al [C5]	1.9	Calcination at 500 °C	4–5	335
1.5Pt/Al [C5]	1.5	Calcination at 800 °C	4–5	207
1.5Pt/Al [LC5]	1.5	Lyophilisation + Calcination at 500 °C	4–5	406

[a] Wt% of metal measured by inductively coupled plasma emission spectrophotometry (ICP).
[b] Calculated as the medium value from transmission electron microscopy (TEM) data.

dissociation onto Pt nanoparticle even at low H_2 concentrations on the catalytic surface.

All these observations demonstrate that physical (i.e. surface area, micro- and/or mesoporosity, particle size) and mainly chemical properties (i.e. water adsorption capacity, acid/base character) of oxides used as supports have an enormous influence on the final catalytic activity of Me-catalysts, but they are not totally determining. In this sense, it is here proved that the modifications of the interactions between the support and the corresponding metal nanoparticle could improve the catalytic activity of Me-based materials depending on the type of metal involved.

3.4. Influences of γ-Al_2O_3 pre-treatments on the catalytic activity of Pt/Al_2O_3 catalysts

Different Pt/γ-Al_2O_3 samples (named as Pt/Al) were prepared using a high surface area γ-Al_2O_3 synthesized in our laboratory as support. This γ-Al_2O_3 was submitted before Pt incorporation to two different treatments: (i) lyophilisation [L], and (ii) calcination at 500 °C [C5] or 800 °C [C8]. Another γ-Al_2O_3 sample was also prepared by combining both lyphilization and posterior calcination at 500 °C processes. In general, lyophilised γ-Al_2O_3 presented higher surface area (420–440 $m^2\ g^{-1}$) than calcined samples (≈300 and ≈400 $m^2\ g^{-1}$ for 800 and 500 °C calcination temperatures, respectively). Simple pH measurements of aluminas revealed that lyophilised sample (pH ≈4.3) presented lower pH values than calcined samples (pH around 6.1–6.2). Pt/Al samples containing approximately 1.0, 1.5, and 2.0 wt% of Pt on alumina were synthesized and adequately characterized (i.e. TG–DTA analyses, XRD, TEM, chemical analyses, among others) and their main textural and physical properties are summarized in Table 3. All Pt/Al materials showed metal particle diameters around 4–5 nm with a narrow distribution and homogeneously dispersed on alumina surface (TEM images not shown). X-ray diffraction patterns of reduced samples (data not shown) showed the characteristic reflections peaks of Pt (at 2θ = 39.9, 46.7, 67.8, 81.8, and 86.0) which evidenced the presence of Pt^0 metallic species on solids. At the same time, XRD diffractograms revealed that the γ-Al_2O_3 structure remained almost unaltered after the reduction treatment in each case. All Pt/Al samples were calcined at 400 °C and then reduced at 350 °C before their catalytic evaluation in the reductive amination of cyclohexanone with piperidine (model reaction), the results being shown in Fig. 7.

In general, the catalytic results of Fig. 7 revealed that Pt/Al calcined samples were much more active than Pt/Al lyophilised ones. Thus, Pt/Al [C5] and Pt/Al [C8] materials presented moderate to high amine conversions (Fig. 7(A)) with selectivities to the tertiary amine at 7 h of reaction upper than 95% in all the cases (Fig. 7(B)). Interestingly, 1Pt/Al [C5] was the most active sample (TON = 1685) followed by the corresponding 1Pt/Al [C8] sample (TON = 1368), always with excellent *tert*-amine selectivity values (≥95%). In both cases, increasing in the amount of Pt on samples produced a slightly increase in the amine conversion from 43 to 50% in the case of 1 and 2Pt/Al [C5], and from 35 to 40 in the case of 1 and 2Pt/Al [C8] samples. Nevertheless, comparison of the total catalytic activity achieved with 1 and 2Pt/Al samples demonstrated that higher Pt contents let to lower TON values (Fig. 7(A)). Thus, the right Pt content on samples could be established in the range of 1.0–1.5 wt%, incorporation of more Pt not producing beneficial effects. Additionally, it is clearly showed that alumina pre-treated by calcination at 500 °C before Pt incorporation produces more active catalysts than those obtained by calcination at 800 °C. In the case of lyophilised samples, both 1Pt/Al [L] and 1.5Pt/Al [LC5] catalysts showed amine conversions at 7 h of reaction inferior to 20% (TON = 555 and 448, respectively), this demonstrating that lyophilisation pre-treatmnet of alumina before metal deposition produces Pt-catalysts with low activity for the reductive amnination reaction.

All these observations let us to conclude that the type of alumina support pre-treatment have a great impact on the final catalytic activity of Pt/γ-Al_2O_3 materials. While lyophilisation produced high surface area γ-Al_2O_3 with high content of hydroxyl groups onto the solid surface, calcination treatment decreased the amount of these exposed hydroxyl species giving a less acidic support surface. Thus, an adequate calcination process at 500 °C (or even

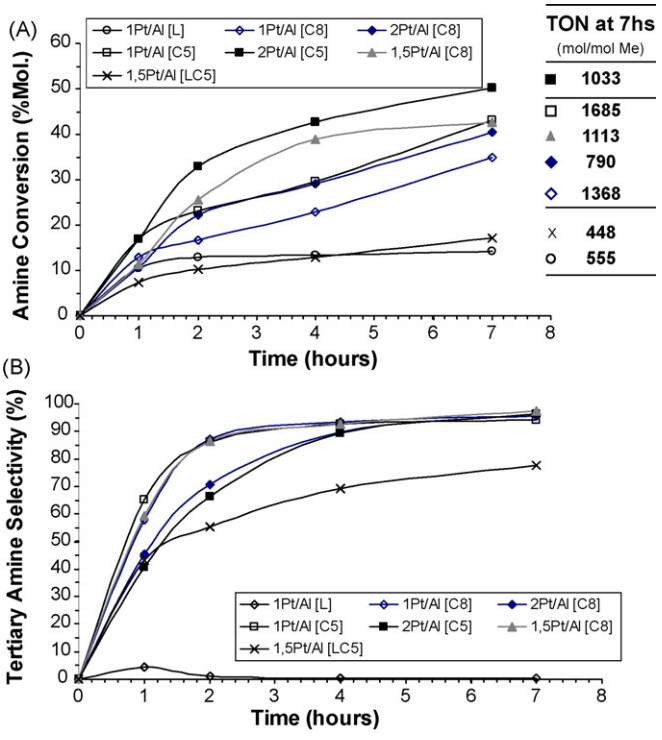

Fig. 7. Effects of alumina pre-treatments on the catalytic activity of Pt/Al_2O_3 samples in the reductive amination of cyclohexanone with piperidine (at 100 °C and P_{H_2} = 5 bar during 7 h); (A) amine conversion (%mol.), and (B) tertiary amine selectivity (%mol.).

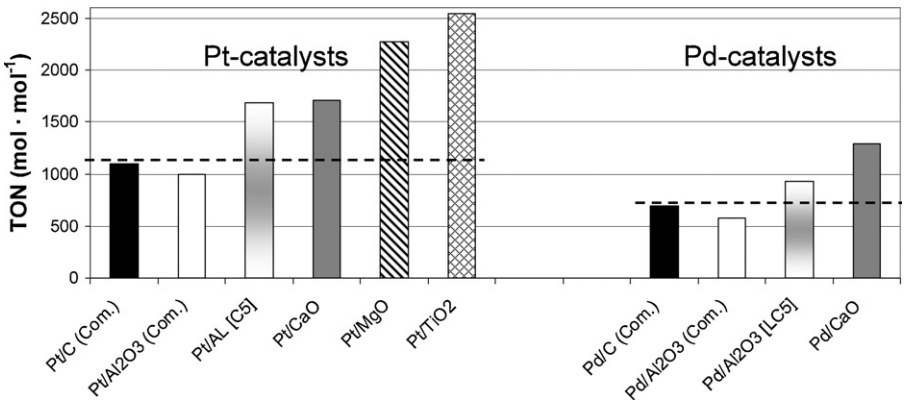

Fig. 8. Comparative catalytic activity (TON, mol mol^{-1}) of Pt and Pd catalysts in the reductive amination of cyclohexanone with piperidine (0.005 mmol of Pt or 0.009 mmol of Pd, at 100 °C and P_{H_2} = 5 bar during 7 h).

superior) guarantied the preparation of efficient Pt/γ-Al_2O_3 catalysts for the selective reductive amination of ketones achieving amine conversions around 50% (TON = 1685) and *tert*-amine selectivities upper than 95%. These results were practically two-fold higher than to those observed with the 1.0 wt% Pt/Al_2O_3 sample (TON = 885) preliminary tested by HT experimentation (Table 1), this showing the great enhancement of catalytic achieved after a more detailed alumina pre-treatment study. Moreover, these excellent catalytic results were also higher than those reached with Pt/Al_2O_3 commercial catalysts already commented in Section 3.1 (Figs. 1 and 2). On the contrary, it was also observed that lyophilisation pre-treatment of alumina produced Pt/Al_2O_3 samples with low catalytic activity. Nevertheless, when this lyophilized alumina was used as support for preparation of a Pd supported material (1.5Pd/Al [LC5] sample); a marked enhancement of catalytic activity (TON value from 727 to 924) was observed. This fact demonstrates once again that physical and chemical properties of oxides used as supports have an enormous influence on the final catalytic activity of Me-catalysts, but also that support properties modifications could be beneficial or detrimental to the catalytic activity found depending on the type of metal to be incorporated.

3.5. Comparative analyses of the Pt and Pd prepared materials with commercial catalysts

One of the objectives of this research work was to design efficient Pt and Pd catalysts for the selective reductive amination of ketones by studying different oxide supports and their properties in order to enhance the results obtained with standard commercial catalysts. Comparison of the catalytic activity values (TON, mol mol^{-1}) obtained with Pt and Pd commercial catalysts and those achieved with the best Pt and Pd nanoparticle supported catalysts prepared in this study for the reductive amination of cyclohexanone with piperidine are detailed in Fig. 8. In all the cases, selectivities to the tertiary amine were upper than 95%. As can be seen, the improved Pt/TiO_2 and Pt/MgO samples showed excellent catalytic activities (TON = 2541 and 2274), these values being practically 2.5 and 2 times, respectively, higher to the best Pt commercial catalysts tested Pt/C, TON = 1102), and of course superior to those of the Pt/Al_2O_3 commercial sample. Besides, the improved both Pt/CaO and 1Pt/Al [C5] catalysts presented TON values 1.5 times higher than those obtained with the Pt/C commercial sample. These results clearly probe the exit of the enhancement of Pt supported samples catalytic activity in this study. The same can be concluded with respect to the Pd-based materials, although all Pd-catalysts showed lower catalytic activities than their Pt-counterparts. Thus, the improved Pd/CaO presented TON values practically two-fold higher than those obtained with the best Pd/C commercial sample. The Pd/Al_2O_3 [LC5] prepared sample had TON values quite superior to those of the Pd/C catalyst, and at least 1.5 times higher than its commercial analogous, the Pd/Al_2O_3 (Com.) sample.

The leaching of platinum was investigated in both Pt/TiO_2 and Pt/MgO catalysts by filtering off the reaction mixtures after 7 h of catalytic reactions, both solid catalyst and liquid being recovered separately. When a new reaction was started by adding fresh reactants to the recovered liquid, any additional conversion was detected. This is consistent with the fact that the reaction does not proceed in homogeneous phase. Besides, ICP measurements of Pt contents on recovered liquids revealed that less than 0.1 wt% of the total catalyst weight (thus, 10 wt% of the initial amount of Pt on the solid) was transferred to the liquids in both cases, this being consistent with the determined amount of Pt remaining on Pt/TiO_2 (≈0.9 wt%) and Pt/MgO (≈1.0 wt%) used catalysts. From these results we concluded that the reductive amination reaction over Pt-catalysts occurs in a heterogeneous way, although a low leaching of Pt species was detected after reaction meaning that the catalyst would tend to deactivate upon successive recycling. In this sense, recycling tests were performed with the Pt/TiO_2 sample to corroborate leaching issues during at least 3 consecutive re-uses (Table S2 in supporting information), results demonstrating that Pt content in solids remains practically invariable after second and third re-use of the catalyst.

Summarising, it is possible to improve the catalytic activity of metal nanoparticles supported on oxides by a combination of the appropriate support pre-treatment together with the adequate post-synthesis reduction process, this making possible a strong metal-support interaction (SMSI) on solid surfaces. This interaction improve hydrogen dissociation capacity of metal particle, while the adequate support properties facilitates reactant adsorption onto the solid surface, and consequently, accelerates reduction reaction which is the limiting step in this process.

4. Conclusions

Different multi-functional catalysts (i.e. redox and acid/base capacities) based on Pt, Pd, and also Au nanoparticles supported on different metal oxides have been here developed by combination of HT experimentation and rational design of materials. Rapid catalytic screening of the prepared Me-catalysts in the liquid phase reductive amination of ketones with a secondary amine allowed us to the preliminary selection of the most promising Pt and Pd supported materials for a more detailed study. In general, Pt-catalysts have shown to be more active in the reductive amination than the corresponding Pd counterparts, while Au-based materials have presented very low catalytic activities. Thus, Pt/TiO_2 sample has proved

to be the most efficient catalyst with amine conversions upper than 50% (TON = 2033) followed by Pt/MgO, Pt/CaO, and Pt/Al_2O_3 in order of reactivity, selectivity to the tertiary amine being >95% in all these cases. For Pd-catalysts, Pd/CaO and Pd/Al_2O_3 have shown the better catalytic activities always with high *tert*-amine selectivity (>95%). Enhanced catalytic activities have obtained with Pt supported on TiO_2, MgO and CaO, by increasing the temperature of the reduction pre-treatment of Me-catalysts before catalytic experiment, the catalytic behaviour of Pt-catalysts thus prepared being quite superior to those observed with Pt/C and Pt/Al_2O_3 commercial samples. Moreover, our study has also demonstrated that the catalytic activity of Pt/γ-Al_2O_3 samples was strongly influenced by the alumina pre-treatment conditions before metal incorporation, but also by the post-synthesis treatments before catalytic evaluation. As a general conclusion, it has been shown here that the catalytic activity in the reductive amination reaction observed with Pt- and Pd-catalysts mainly depends on: (i) the type of support, (ii) the chemicals and physical properties of support, and also (iii) the type of metal incorporated. More importantly, the activity of the Pt-catalysts strongly depends on the strong metal-support interaction (SMSI) occurring at the interface between metal nanoparticle and support surface, this being applicable to more or less reducible oxides, as well as non-reducible oxides, used as supports. Further investigations are now being carried out to establish the corresponding trends and the more adequate pre- or post-synthesis treatment conditions for catalytic activity improvement of the Pd-based materials.

Acknowledgments

Authors gratefully acknowledge financial support by Generalitat Valenciana (GVPRE-2008-109) and Ministerio de Ciencia e Innovación of Spain (CTQ-2008-06446).

Appendix A. Supplementary data

Supplementary data associated with this article can be found, in the online version, at doi:10.1016/j.cattod.2010.08.011.

References

[1] J.J. Birtill, J. Mol. Catal. A: Chem. 305 (2009) 183.
[2] Y.S. Higassio, T. Shoji, Appl. Catal. A: Gral. 221 (2001) 197.
[3] N.R. Candeias, C.A.M. Afonso, J. Mol. Catal. A: Chem. 242 (2005) 195.
[4] S. Shimizu, T. Niwa, T. Shoji, Koei Chemical Co. Ltd., JP 02011577. (1988).
[5] V.R. Rani, N. Srinivas, S.J. Kulkarni, K.V. Raghavan, J. Mol. Catal. A:Chem. 187 (2002) 237.
[6] K.G. Liu, A.J. Robichaud, Tetrahedron Lett. 46 (2005) 7291.
[7] P. Vairaprakash, M. Periasamy, J. Org. Chem. 71 (2006) 3636.
[8] T. Mallat, A. Baiker, in: R.A. Sheldon, H. van Bekkum (Eds.), Fine Chemical through Hetereogeneous Catalysis, Wiley-VCH, Weinheim, 2001, p. 247.
[9] A. Baiker, J. Kijenski, Catal. Rev. Sci. Eng. 27 (1985) 653.
[10] A. Corma, T. Ródenas, M.J. Sabater, Chem. Eur. J. 16 (2010) 254.
[11] M. Haniti, S.A. Hamid, J.M.J. Williams, Chem. Commun. (2007) 725.
[12] K. Fujita, Z. Li, N. Ozeki, R. Yamaguchi, Tetrahedron Lett. 44 (2003) 2687.
[13] D. Gnanamgari, E.L.O. Sauer, N.D. Schley, C. Butler, C.D. Incarvito, R.H. Crabtree, Organometallics 28 (2009) 321.
[14] P. Dolezal, O. Machalicky, M. Pavelek, P. Kubec, K. Hradkova, R. Hrdina, R. Sulakova, Appl. Catal. A: Gral. 286 (2005) 202.
[15] D.M. Roundhill, Chem. Rev. 92 (1992) 1.
[16] Y. Watanabe, Y. Tsuji, Y. Ohsugi, Tetrahedron Lett. 22 (28) (1981) 2667.
[17] C. González-Arellano, A. Corma, M. Iglesias, F. Sánchez, Inorg. Chim. Acta 357 (2004) 3071.
[18] C. González-Arellano, A. Corma, M. Iglesias, F. Sánchez, Adv. Synth. Catal. 346 (2004) 1316.
[19] T.F. Baumann, A.E. Gash, S.C. Chinn, A.M. Sawvel, R.S. Maxwell, J.H. Satcher, Chem. Mater. 17 (2005) 395.
[20] J.Y. Chane-Ching, F. Cobo, D. Aubert, H.G. Harvey, M. Airiau, A. Corma, Chem. Eur. J. 11 (3) (2005) 979.
[21] S. Carrettin, P. Concepcion, J.M. Lopez-Nieto, V.F. Puntes, A. Corma, Angew. Chem. Int. Ed. 43 (19) (2004) 2538.
[22] C. Aprile, A. Corma, M.E. Domine, H. García, C. Mitchell, J. Catal. 264 (2009) 44.
[23] A. Morlang, U. Neuhausen, K.V. Klementiev, F.-W. Schütze, G. Miehe, H. Fuess, E.S. Lox, Appl. Catal. A: Gral. 60 (2005) 191.
[24] J. Lengyel, Z. Cvengrošová, J. Cvengroš, Petrol. Coal 51 (3) (2009) 216.
[25] M.A. Aramendía, J.A. Benítez, V. Borau, C. Jiménez, J.M. Marinas, J.R. Ruiz, F.J. Urbano, Colloids Surf. A: Physicochem. Eng. Aspects 168 (2000) 27.
[26] M.A. Aramendía, J.A. Benítez, V. Borau, C. Jiménez, J.M. Marinas, J.R. Ruiz, F. Urbano, Langmuir 15 (1999) 1192.
[27] S. Abbet, U. Heiz, in: C.N.R. Rao, A. Müller, A.K. Cheetham (Eds.), "The Chemistry of Nanomaterials. Synthesis Properties and Applications", Vol.2, Wiley-VCH, Weinheim, 2005, p. 551.
[28] J. Adamiec, J.A. Szymura, S.E. Wanke, Stud. Surf. Sci. Catal. 75 (1993) 1405.
[29] Y. Li, Y. Fan, H. Yang, B. Xu, L. Feng, M. Yang, Y. Chen, Chem. Phys. Lett. 372 (2003), 160 (and refs. there in).
[30] T. Lopez, I. Garcia-Cruz, R. Gomez, Mater. Chem. Phys. 36 (3–4) (1994) 222.